Ultimate terahertz field enhancement of single nanoslits

Young-Mi Bahk,[1,*] Sanghoon Han,[1,†] Jiyeah Rhie,[1] Joohyun Park,[2] Hyeongtag Jeon,[2,3] Namkyoo Park,[4] and Dai-Sik Kim[1,‡]

[1]*Department of Physics and Astronomy and Center for Atom Scale Electromagnetism, Seoul National University, Seoul 08826, Korea*

[2]*Department of Nanoscale Semiconductor Engineering, Hanyang University, Seoul 04763, Korea*

[3]*Division of Materials Science and Engineering, Hanyang University, Seoul 04763, Korea*

[4]*Photonic Systems Laboratory, Department of Electrical and Computer Engineering, Seoul National University, Seoul 08826, Korea*

(Received 21 November 2016; revised manuscript received 23 January 2017; published 21 February 2017)

A single metallic slit is the simplest plasmonic structure for basic physical understanding of electromagnetic field confinement. By reducing the gap size, the field enhancement is expected to first go up and then go down when the gap width becomes subnanometer because of the quantum tunneling effects. A fundamental question is whether we reach the classical limit of field enhancement before entering the quantum regime, i.e., whether the quantum effects undercut the highest field enhancement classically possible. Here, by performing terahertz time domain spectroscopy on single slits of widths varying from 1.5 nm to 50 μm, we show that ultimate field enhancement determined by the wavelength of light and film thickness can be reached before we hit the quantum regime. Our paper paves way toward designing a quantum plasmonic system with maximum control yet without sacrificing the classical field enhancements.

DOI: 10.1103/PhysRevB.95.075424

Local field enhancement and confinement of electromagnetic waves in nanosize volumes are central to diverse applications in nano-optics, such as single molecule detection [1–4], optical manipulation [5,6], and nanoscale nonlinear optics [7–10]. For a nanogap consisting of two metals separated by a nanometer distance, the current is induced in the metal surfaces by the incident light and the electric charges accumulate near the sharper edges of the metals due to charge continuity. These accumulated charges contribute to enhancing the electric field inside the nanogap, resulting in a voltage drop between two metals that can induce electron tunneling across the gap. Several papers have demonstrated that the local field enhancement in nanogaps increases monotonically with decreasing gap size [11–14] and that it decreases as it enters the quantum regime [15–22] [Fig. 1(a)]. A fundamental question is whether we reach the classical limit of field enhancement before entering the quantum regime [Fig. 1(b)].

The main reason for difficulty in investigating the classical limit of field enhancement is the treatment of complicated metallic systems with a finite dielectric constant and nonideal shape of the structure. This led us to design a set of experiments in which all electromagnetic waves funnel through the nanogaps formed by the simplest plasmonic structure. In this paper, terahertz electric field enhancement of a single slit is monitored as we decrease the gap size from 50 μm to 1.5 nm. The investigation of the induced current and charge distribution in metal films allows us to understand the physical processes of reaching the largest possible field enhancement in a slit structure, determined by the wavelength of light and the gap thickness.

An infinitely long single slit formed by two metal films simplifies the interaction between electromagnetic waves with subwavelength apertures [12,23,24]. Since the metal is considered a perfect electric conductor (PEC) due to a large dielectric constant for long-wavelength waves such as terahertz waves and microwaves, all electromagnetic waves can squeeze through the metal slits without any strays because of a large contrast of dielectric constant [12,25,26]. This allows us to simplify the funneling process, enabling a deep understanding of the giant field enhancement in nanogaps, as well as many potential applications in plasmonics [27–36].

We manufactured millimeter-long single slits on a gold (Au) film deposited onto a sapphire substrate with various gap sizes from 50 μm down to 1.5 nm, as shown in Fig. 2(a). The samples are made by two fabrication techniques. One method uses a focused ion beam for the slits with a gap size from 50 μm to 200 nm. The other method is atomic layer lithography for gaps of a few nanometers filled with aluminum oxide (Al_2O_3) as an insulating layer, as shown in the inset of Fig. 2(a) [14]. This advanced lithography technique allows us to make a high aspect ratio between gap thickness (h) and gap size (w): $h/w \gg 1$. All samples have an effective gap thickness h [36] of around 150 nm, which is the subskin depth of the metal ($\delta_{Au} \sim 250$ nm for 0.1 THz), and a slit length l of 2 mm, which is considered an infinite slit for a 1 by 1 mm aluminum aperture as a reference. Figure 2(b) and (c) are top views of scanning electron microscope (SEM) images for the samples of 2 μm (top), 200 nm (middle), and 2 nm (bottom) gaps and cross-sectional views of SEM images for 10, 5, 2.5, and 1.5 nm gaps (from left to right), respectively.

Figure 3(a) shows representative time traces of the transmitted terahertz electric field for a 5 nm gap sample (red) and bare sapphire substrate (black) with a 1 by 1 mm aluminum aperture. To take into account the transmitted signal only through the gap, the contribution of the transmitted field of Au film is subtracted in the sample data (see Supplemental Material [37]). As shown in Fig. 3(b), the properties of transmission through the single slits are experimentally characterized by Fourier-transformed normalized transmitted amplitude [Fig. 3(b), left

*Present address: Max Planck Institute for the Structure and Dynamics of Matter, 22761 Hamburg, Germany.

†Present address: Semiconductor Research and Development Center, Samsung Electronics, Gyeonggi-Do 18448, Korea.

‡Corresponding author: dsk@phya.snu.ac.kr.

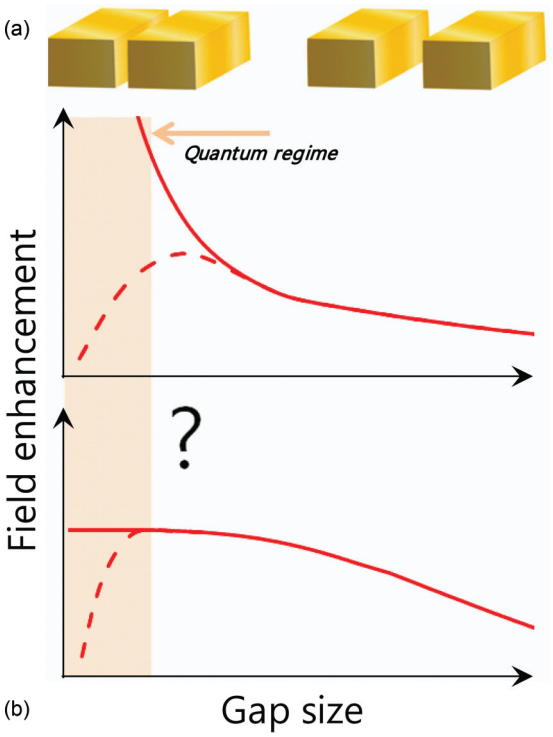

FIG. 1. Schematics of the field enhancement change in the metallic nanogap structure. (a) By reducing the gap size, the field enhancement is expected to first go up and then go down when the gap size becomes subnanometer because of the quantum tunneling effect. (b) A fundamental question is whether we reach the classical limit of field enhancement before entering the quantum regime.

axis], defined as $t = E_{\mathrm{gap}}(\omega)/E_{\mathrm{ref}}(\omega)$, where E_{gap} is the transmitted electric field amplitude through the sample with the aperture and E_{ref} is that only through the substrate with the same aperture. In the graph, we observe two salient features. First, the transmission of the single nanoslit increases with decreasing frequency, describing a $1/f$ dependence, presented

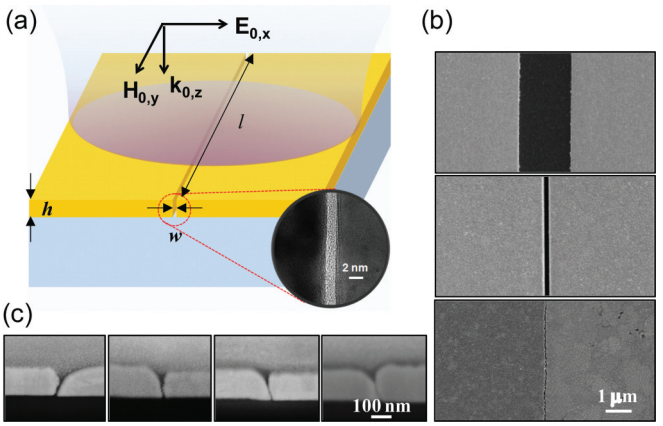

FIG. 2. (a) Schematic of an infinite single slit. The structure is illuminated by normally incident p-polarized terahertz waves. The inset is a transmission electron microscopy (TEM) image of a 1.5 nm Al_2O_3 gap fabricated by atomic layer lithography. (b) Top views of SEM images for single slits with three gap sizes: $w = 2$ μm (top), 200 nm (middle), and 2 nm (bottom). (c) Cross-sectional views of SEM images for 10, 5, 2.5, and 1.5 nm gaps (from left to right).

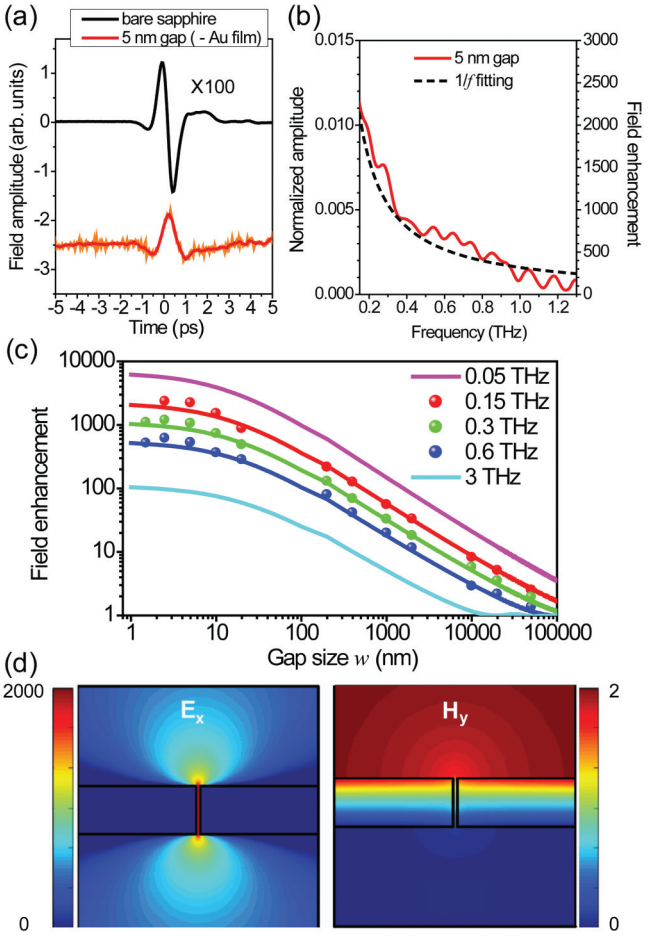

FIG. 3. (a) Time traces of the transmitted terahertz electric field through a sapphire substrate with a 1 by 1 mm aluminum aperture (black) and a 5 nm gap sample with the same aperture (red). The direct transmission of Au film is subtracted in the sample data. (b) Normalized transmitted amplitudes (left axis) and field enhancement (right axis) of a 5 nm gap as a function of frequency. The fit (black dashed line) indicates $1/f$ dependence. (c) Field enhancement as a function of gap size w for several frequencies. The solid lines are the theoretical calculation of the modal expansion formalism. (d) Horizontal electric field (left) and magnetic field (right) around a 1.5 nm gap with an area of 500 by 500 nm simulated by FDTD. The frequency is fixed at 0.15 THz.

as a dotted line. This implies a capacitor-like charging of the nanogap because the induced total charges are inversely proportional to the frequency, $Q_{\mathrm{ind}} \sim I_0/\omega$, for an alternating current source of terahertz frequencies $I = I_0 e^{-i\omega t}$ (ω is the angular frequency of the incident light) [12]. Second, around 1% transmission at 0.15 THz is tremendously high when one considers the extremely small gap-to-aperture area ratio of only $\beta = 5\,\mathrm{nm}/1\,\mathrm{mm} = 5 \times 10^{-6}$. Therefore, a field enhancement inside a 5 nm gap of $t/\beta \sim 2000$ is extracted by the Kirchhoff integral formalism, as shown in the right axis of Fig. 3(b) [29].

Figure 3(c) shows electric field enhancement as a function of gap size for different frequencies. The solid lines indicate theoretical calculation of the modal expansion formalism based on the PEC model, which is valid for the terahertz

frequency regime [30]. We have checked that both two-dimensional finite-difference time domain (FDTD) simulation and PEC modal expansion provide essentially the same results of the field enhancement factor [36]. The measured data show that the field enhancement increases and eventually saturates as the gap size decreases from 50 μm to 1.5 nm for all frequencies. This tendency is in agreement with the theoretical calculations. Since the maximum electric field of the incident terahertz pulse is around $E_0 \sim 30\,\mathrm{V/cm}$, the induced transient voltage across a 1.5 nm gap is only about $V_{\mathrm{gap}} \sim 3.2\,\mathrm{mV}$ despite the giant field enhancement of around 1000. Therefore, the quantum effect of electron tunneling is negligible in this weak field regime [21,22]. Our experimental results demonstrate that the terahertz field enhancement in a nanoslit can saturate before the quantum effects become active, in contrast to recent papers on the optical regime that have demonstrated monotonically increasing resonant plasmonic field enhancement with decreasing gap size of a nanoparticle dimer and quenching by the quantum effect of tunneling and nonlocal screening [38].

Our results prove the existence of the largest possible field enhancement achieved by two metal films forming a nanogap in the classical electromagnetic description that provides significant information for the development of plasmonic devices and applications, such as chemical and biological molecule sensing in infrared, terahertz, and microwave. Figure 3(d) gives the electric (left) and magnetic (right) field distribution around a 1.5 nm gap in 150-nm-thick Au film simulated with FDTD analysis at a wavelength of 2 mm ($f = 0.15\,\mathrm{THz}$). The results reveal the expected behavior that the horizontal electric field is strongly focused and enhanced up to 2000 times inside the gap (intensity enhancement of 4 million) while the magnetic field is continuously decreasing and spreading inside the metal with no enhancement in the gap.

As we indicate in Fig. 4(a), three regimes are identified for different values of gap size w: (i) $w \ll h\,(\ll \lambda)$, (ii) $w \sim h\,(\ll \lambda)$ and (iii) $w \gg h$ and $w < \lambda$. . We first discuss the two extreme regimes. The first regime arises for $w \ll h\,(\ll \lambda)$ where the enhancement does not increase drastically, showing a saturation behavior. The saturation value for the field enhancement can be estimated by a capacitor model describing the nanoslit with a capacitance $C = \varepsilon_{\mathrm{gap}} A/w$, where $A = hl$ is the area of the slit edge and $\varepsilon_{\mathrm{gap}}$ is the permittivity of the gap material. Since the incident magnetic field H_0 is related to E_0 by the vacuum impedance of free space Z_0 and it induces the surface current $\vec{K}_0 (= \vec{J}_0 \times h) = \hat{n} \times (2\vec{H}_0)$ in PEC, one can estimate the induced total charges $Q_{\mathrm{ind}} = \varepsilon_0 \frac{\lambda}{\pi h} A E_0$ by the charge conservation law: $\nabla \cdot \vec{K} + \frac{\partial \sigma}{\partial t} = 0$, where σ is the surface charge density. With the approximation that almost all charges are accumulated at the edges of the slit, the field enhancement factor of a nanoslit for a given h, $\frac{E_{\mathrm{gap}}}{E_0} = \frac{V_{\mathrm{gap}}/w}{E_0} = \frac{\lambda}{(\varepsilon_{\mathrm{gap}}/\varepsilon_0)\pi h}$, was initially derived in 2005 [39]. This was rederived in 2009 and 2014 [27,40]. For comparison with the experimental data, the field enhancement normalized by the substrate $\frac{n_{\mathrm{sub}}+1}{2} \frac{\lambda}{(\varepsilon_{\mathrm{gap}}/\varepsilon_0)\pi h}$, where n_{sub} is the refractive index of the sapphire substrate, is depicted with a red dotted line in Fig. 4(a). This implies that we experimentally reached a fully capacitive charging regime with a high aspect ratio

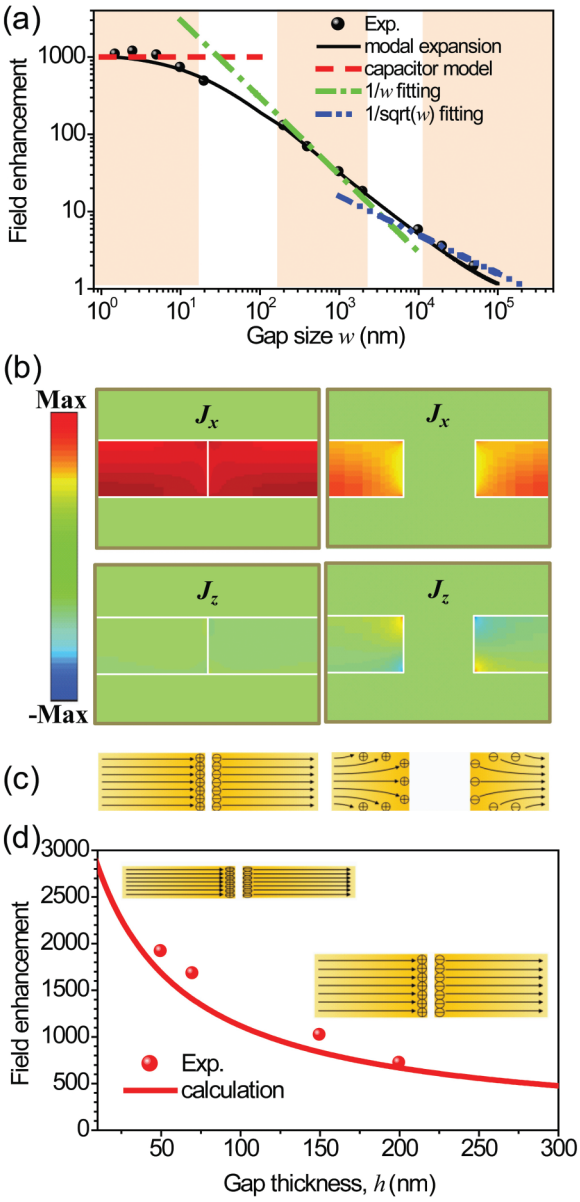

FIG. 4. (a) Field enhancement as a function of the gap size w. Transition of the field enhancement by decreasing the gap size w at 0.3 THz. The gap thickness h is fixed at 150 nm. Three regimes are identified for different values of w. The black dot is experimental data, and the black solid line is the result by modal expansion. For the regime of $w \ll h\,(\ll \lambda)$, the field enhancement shows a saturation behavior reaching to the ultimate limit estimated by a simple capacitor model (red line). The regime for $w \sim h\,(\ll \lambda)$ and that for $w \gg h$ and $w < \lambda$ are close to the dependence of $1/w$ (green line) and $1/\sqrt{w}$ (blue line), respectively. (b) Two components of the induced current density, J_x (top) and J_z (bottom), in 150-nm-thick Au film for w of 200 nm (right) and 1.5 nm (left). (c) Schematics of the induced current density depicted with black arrows in a metal film and the accumulated charges near the slit edges for two gap sizes: $w \sim h\,(\ll \lambda)$ (right) and $w \ll h\,(\ll \lambda)$ (left). (d) Electric field enhancement of a 5 nm gap as a function of the gap thickness h. The solid line is the calculation of modal expansion. The schematics indicate that $1/h$ dependence of the field enhancement results from an increased surface charge density due to the constant value of the induced surface current K.

nanoslit ($h/w \gg 1$) fabricated by atomic layer lithography. In parallel, the same equation of electric field enhancement is derived from analytical calculation of PEC modal expansion, adding approximations of $h/w \gg 1$, where $w \ll \lambda$ and $h \ll \lambda$ (Supplemental Material [37]).

The third regime ($w \gg h$ but $w < \lambda$) in which field enhancement is closely described by a dependence of $1/\sqrt{w}$ can be explained by two Sommerfeld half planes without coupling between the two metal films. For a Sommerfeld half plane, the electric field is proportional to the inverse square root of x, where x is the distance from the slit edge [41]. Considering a single slit as two Sommerfeld half planes without any coupling effect, the averaged electric field inside the gap corresponding to the field enhancement is proportional to the inverse square root of w. The second regime ($w \sim h$ ($\ll \lambda$)) in which the field enhancement is close to the fitting of $1/w$ is the intermediate regime, in which two metal films start to couple strongly before entering the fully capacitive charging regime [12,13].

In order to understand the physical process of reaching the saturation limit of field enhancement, we plotted two components of induced current density, J_x (top) and J_z (bottom), in metal films for a gap size of 200 nm (right) and 1.5 nm (left) in Fig. 4(b). In the simulation, the metal thickness is fixed at 150 nm, giving the aspect ratios h/w of 0.75 and 100, respectively. With J_x and J_z, we schematically present the induced current and accumulated charges near the gaps in Fig. 4(c). Again, the induced total charges are fixed. For a 200 nm gap ($w \sim h$) [Fig. 4(c), right], the charges are not perfectly accumulated at the slit edges but are slightly spread away from the edges due to the current distortion near the gap. Since the spread distance is around the gap size, the field enhancement strongly depends on the gap size when $w \sim h$. This gives rise to a stronger field enhancement of a smaller gap presented in the intermediate regime, as shown in Fig. 4(a). For a 1.5 nm gap ($w \ll h$) [Fig. 4(c), left], the charges are mostly accumulated at the slit edges due to an almost straightly flowing surface current resembling that in a metal film without a gap. This also gives us a good prediction of the ultimate field enhancement factor $\frac{E_{\text{gap}}}{E_0} = \frac{\lambda}{(\varepsilon_{\text{gap}}/\varepsilon_0)\pi h}$, derived from the boundary condition of the electric field at a metal surface inside the gap $\varepsilon_{\text{metal}} E_{\text{metal}} = \varepsilon_{\text{gap}} E_{\text{gap}}$ and the calculation of the transmitted electric field inside a metal using thin film approximation $E_{\text{metal}} \sim 2E_0/(\sigma_{\text{metal}} h Z_0)$, where E_{metal} is the electric field inside a bare metal film; $\varepsilon_{\text{metal}}$, and ε_{gap} are permittivities of the metal and gap material, respectively; and σ_{metal} is the conductivity of the metal [42].

To increase the field enhancement in the fully capacitive charging regime, it is necessary to decrease the thickness of metal film h, which results in an increased surface charge density at the slit edges with a fixed surface current K. To verify the description experimentally, we fabricated infinite single slits of a 5 nm gap with four gap thicknesses: $h = 200, 150, 70,$ and 50 nm. Figure 4(d) presents the field enhancement of the 5 nm gap as a function of gap thickness h at the frequency of 0.3 THz. The red dots correspond to the experimental data, well matched with a $1/h$ dependence. The field enhancement is insensitive to the gap thickness for the regime $w \geqslant h$, except for $w \ll h$.

In conclusion, we achieved ultimate terahertz field enhancement in an infinite single slit with sub-10-nm-size gap successfully fabricated by atomic layer lithography. The limit of electric field enhancement determined by the wavelength of light and the gap thickness results from the fully capacitive charging behavior realized by nanogaps with a high aspect ratio between the gap thickness and the gap size. This paper is the first experimental demonstration of the ultimate limit of gap-size-controlled field enhancement in the classical electromagnetic description. We also achieved stronger field enhancement in the regime in which the field enhancement is insensitive to the gap size, using nanogaps formed by thinner metal films. Our deep understanding of the funneling process of electromagnetic waves through the metallic gap provides significant information for the development of plasmonic devices and practical applications in nano-optics and nonlinear plasmonics.

This work was supported by the National Research Foundation of Korea (NRF) Grant funded by the Korea government (MSIP: NRF-2015R1A3A2031768) (MOE: BK21 Plus Program-21A20131111123). Y.-M.B. performed the experiments and analysis and wrote the manuscript based on discussions with S.H., N.P., and D.-S.K. The samples were fabricated by Y.-M.B., J.R., J.P., and H.J. FDTD simulations were performed by S.H. and N.P. The experimental concept was conceived by D.-S.K. All authors reviewed and contributed to the final manuscript.

[1] E. Burstein, Y. J. Chen, C. Y. Chen, S. Lundquist, and E. Tosatti, Solid State Comm. **29**, 567 (1979).
[2] K. Kneipp, Y. Wang, H. Kneipp, L. T. Perelman, I. Itzkan, R. R. Dasari, and M. S. Feld, Phys. Rev. Lett. **78**, 1667 (1997).
[3] S. Nie and S. R. Emory, Science **275**, 1102 (1997).
[4] H. Xu, E. J. Bjerneld, M. Käll, and L. Börjesson, Phys. Rev. Lett. **83**, 4357 (1999).
[5] M. L. Juan, M. Righini, and R. Quidant, Nat. Photon. **5**, 349 (2011).
[6] O. M. Marago, P. H. Jones, P. G. Gucciardi, G. Volpe, and A. C. Ferrari, Nat. Nanotechnol. **8**, 807 (2013).
[7] D. R. Ward, F. Huser, F. Pauly, J. C. Cuevas, and D. Natelson, Nat. Nanotechnol. **5**, 732 (2010).
[8] M. Kauranen and A. V. Zayats, Nat. Photon. **6**, 737 (2012).
[9] Y.-M. Bahk, G. Ramakrishnan, J. Choi, H. Song, G. Choi, Y. H. Kim, K. J. Ahn, D.-S. Kim, and P. C. M. Planken, ACS Nano **8**, 9089 (2014).
[10] J. B. Lassiter, X. Chen, X. Liu, C. Ciracì, T. B. Hoang, S. Larouche, S.-H. Oh, M. H. Mikkelsen, and D. R. Smith, ACS Photon. **1**, 1212 (2014).
[11] I. Romero, J. Aizpurua, G. W. Bryant, and F. J. G. d. Abajo, Optic. Express **14**, 9988 (2006).

[12] M. A. Seo, H. R. Park, S. M. Koo, D. J. Park, J. H. Kang, O. K. Suwal, S. S. Choi, P. C. M. Planken, G. S. Park, N. K. Park, Q. H. Park, and D. S. Kim, Nat. Photon. **3**, 152 (2009).
[13] S. Koo, M. S. Kumar, J. Shin, D.-S. Kim, and N. Park, Phys. Rev. Lett. **103**, 263901 (2009).
[14] X. Chen, H.-R. Park, M. Pelton, X. Piao, N. C. Lindquist, H. Im, Y. J. Kim, J. S. Ahn, K. J. Ahn, N. Park, D.-S. Kim, and S.-H. Oh, Nat. Comm. **4**, 2361 (2013).
[15] J. Zuloaga, E. Prodan, and P. Nordlander, Nano Lett. **9**, 887 (2009).
[16] R. Esteban, A. G. Borisov, P. Nordlander, and J. Aizpurua, Nat. Comm. **3**, 825 (2012).
[17] D. C. Marinica, A. K. Kazansky, P. Nordlander, J. Aizpurua, and A. G. Borisov, Nano Lett. **12**, 1333 (2012).
[18] C. Ciracì, R. T. Hill, J. J. Mock, Y. Urzhumov, A. I. Fernández-Domínguez, S. A. Maier, J. B. Pendry, A. Chilkoti, and D. R. Smith, Science **337**, 1072 (2012).
[19] M. S. Tame, K. R. McEnery, S. K. Ozdemir, J. Lee, S. A. Maier, and M. S. Kim, Nat. Phys. **9**, 329 (2013).
[20] S. F. Tan, L. Wu, J. K. W. Yang, P. Bai, M. Bosman, and C. A. Nijhuis, Science **343**, 1496 (2014).
[21] Y.-M. Bahk, B. J. Kang, Y. S. Kim, J.-Y. Kim, W. T. Kim, T. Y. Kim, T. Kang, J. Rhie, S. Han, C.-H. Park, F. Rotermund, and D.-S. Kim, Phys. Rev. Lett. **115**, 125501 (2015).
[22] J.-Y. Kim, B. J. Kang, J. Park, Y.-M. Bahk, W. T. Kim, J. Rhie, H. Jeon, F. Rotermund, and D.-S. Kim, Nano Lett. **15**, 6683 (2015).
[23] T. Kang, J. Rhie, J. Park, Y.-M. Bahk, J. S. Ahn, H. Jeon, and D.-S. Kim, Appl. Phys. Express **8**, 092003 (2015).
[24] J. S. Ahn, T. Kang, D. K. Singh, Y.-M. Bahk, H. Lee, S. B. Choi, and D.-S. Kim, Optic. Express **23**, 4897 (2015).
[25] M. A. Seo, A. J. L. Adam, J. H. Kang, J. W. Lee, K. J. Ahn, Q. H. Park, P. C. M. Planken, and D. S. Kim, Optic. Express **16**, 20484 (2008).
[26] K. Lee, J. Jeong, Y.-M. Bahk, J. Rhie, I.-K. Baek, B. J. Lee, Y. H. Kang, S. Hong, G.-S. Park, and D.-S. Kim, ACS Photon. **3**, 537 (2016).
[27] J. H. Kang, D. S. Kim, and Q. H. Park, Phys. Rev. Lett. **102**, 093906 (2009).
[28] M. Seo, J. Kyoung, H. Park, S. Koo, H.-S. Kim, H. Bernien, B. J. Kim, J. H. Choe, Y. H. Ahn, H.-T. Kim, N. Park, Q. H. Park, K. Ahn, and D.-S. Kim, Nano Lett. **10**, 2064 (2010).
[29] J. S. Kyoung, M. A. Seo, H. R. Park, K. J. Ahn, and D. S. Kim, Optic. Comm. **283**, 4907 (2010).
[30] F. J. Garcia-Vidal, L. Martin-Moreno, T. W. Ebbesen, and L. Kuipers, Rev. Mod. Phys. **82**, 729 (2010).
[31] A. Novitsky, M. Zalkovskij, R. Malureanu, and A. Lavrinenko, Optic. Comm. **284**, 5495 (2011).
[32] M. Shalaby, H. Merbold, M. Peccianti, L. Razzari, G. Sharma, T. Ozaki, R. Morandotti, T. Feurer, A. Weber, L. Heyderman, B. Patterson, and H. Sigg, Appl. Phys. Lett. **99**, 041110 (2011).
[33] M. Shalaby, J. Fabiańska, M. Peccianti, Y. Ozturk, F. Vidal, H. Sigg, R. Morandotti, and T. Feurer, Appl. Phys. Lett. **104**, 171115 (2014).
[34] H.-R. Park, K. J. Ahn, S. Han, Y.-M. Bahk, N. Park, and D.-S. Kim, Nano Lett. **13**, 1782 (2013).
[35] Y.-G. Jeong, S. Han, J. Rhie, J.-S. Kyoung, J.-W. Choi, N. Park, S. Hong, B.-J. Kim, H.-T. Kim, and D.-S. Kim, Nano Lett. **15**, 6318 (2015).
[36] S. Han, Y.-M. Bahk, N. Park, and D.-S. Kim, Optic. Express **24**, 2065 (2016).
[37] See Supplemental Material at http://link.aps.org/supplemental/10.1103/PhysRevB.95.075424 for a detailed discussion about experimental methods and theoretical calculation.
[38] W. Zhu, R. Esteban, A. G. Borisov, J. J. Baumberg, P. Nordlnader, H. J. Lezec, J. Azipurua, and K. B. Crozier, Nat. Comm. **7**, 11495 (2016).
[39] The field enhancement factor calculated by the capacitor model was mentioned in an online document written by D.-S.K. in 2005 (http://nanooptics.snu.ac.kr/wordpress/publication/infinite_slits-capacitor_model_dsk.pdf).
[40] J. Lin, S.-H. Oh, H.-M. Nguyen, and F. Reitich, Optic. Express **22**, 14402 (2014).
[41] M. Born and E. Wolf, *Principles of Optics* (Cambridge University Press, 1999).
[42] J. D. Jackson, *Classical Electrodynamics* (John Wiley & Sons, 2001).